Available online at www.sciencedirect.com
ScienceDirect
Solar Energy 84 (2010) 2219–2229
SOLAR ENERGY
www.elsevier.com/locate/solener

A novel multi-model neuro-fuzzy-based MPPT for three-phase grid-connected photovoltaic system

Aymen Chaouachi *, Rashad M. Kamel, Ken Nagasaka

Department of Electronic and Information Engineering, Tokyo University of Agriculture and Technology, 2-24-16, Nakamachi, Koganei-shi, Tokyo 184-8588, Japan

Received 8 March 2010; received in revised form 9 July 2010; accepted 13 August 2010
Available online 29 September 2010

Communicated by: Associate Editor Elias Stefanakos

Abstract

This paper presents a novel methodology for Maximum Power Point Tracking (MPPT) of a grid-connected 20 kW photovoltaic (PV) system using neuro-fuzzy network. The proposed method predicts the reference PV voltage guarantying optimal power transfer between the PV generator and the main utility grid. The neuro-fuzzy network is composed of a fuzzy rule-based classifier and three multi-layered feed forwarded Artificial Neural Networks (ANN). Inputs of the network (irradiance and temperature) are classified before they are fed into the appropriated ANN for either training or estimation process while the output is the reference voltage. The main advantage of the proposed methodology, comparing to a conventional single neural network-based approach, is the distinct generalization ability regarding to the nonlinear and dynamic behavior of a PV generator. In fact, the neuro-fuzzy network is a neural network based multi-model machine learning that defines a set of local models emulating the complex and nonlinear behavior of a PV generator under a wide range of operating conditions. Simulation results under several rapid irradiance variations proved that the proposed MPPT method fulfilled the highest efficiency comparing to a conventional single neural network and the Perturb and Observe (P&O) algorithm dispositive.

Keywords: Neuro-fuzzy; MPPT; Multi-model; Grid-connected; Photovoltaic

1. Introduction

The Kyoto agreement on global reduction of greenhouse gas emission has prompted interest on renewable energy systems worldwide. Nowadays photovoltaic energy is one of the most popular renewable sources since it is clean, inexhaustible and requires little maintenance. However, it still presents a vast area of competition comparing to conventional energy resources due to its high cost and low efficiency during energy conversion. Regarding to this, it is necessary to optimize the performance of PV systems through the operation of conversion systems to increase the output efficiency of the overall system (Enrique et al., 2007; Chua and Chen, 2009). This approach is commonly named as Maximum Power Point Tracking (MPPT), several methods are referred in the bibliography: the P&O method is the most commonly used in practice due to its simplicity and ease of implementation (Enrique et al., 2010), however, this algorithm can fail or oscillate around the Maximum Power Point (MPP) under sudden sunlight changes (Hohm and Ropp, 2003; Salas et al., 2006). Incremental conductance is also commonly used as it can overcome some aspects of the P&O algorithm instabilities. Nevertheless this method involves current and voltage differentiation which requires a relatively complex decision making process and therefore needs more complex calculation capacity and memory (Esram and Chapman, 2007). More recently, Artificial Neural Network (ANN) techniques are being employed for photovoltaic applications, mainly because of their symbolic reasoning, flexibility

* Corresponding author. Tel./fax: +81 42 388 7481.
E-mail addresses: A.chaouachi@gmail.com (A. Chaouachi), r_m_kamel@yahoo.com (R.M. Kamel), bahman@cc.tuat.ac.jp (K. Nagasaka).

0038-092X/$ - see front matter © 2010 Elsevier Ltd. All rights reserved.
doi:10.1016/j.solener.2010.08.004

Nomenclature

Photovoltaic parameters superscripted with "M" refers to a PV module while those superscripted with "C" are referring to a solar cell and each parameter under scripted with "o" refers to standard conditions

e	electron charge, $e = 1.602 \times 10^{19}$ (C)
I_d	diode current (A)
I_0	reverse saturation current (A)
I_{sc}	short-circuit current (A)
$I^M_{sc_o}$	short-circuit current under standard conditions (A)
$V^M_{OC_o}$	open voltage under standard conditions (V)
V_T	thermal voltage in the semiconductor (V)
$P^M_{max_o}$	power under standard conditions (W)
N_S	cells in series in a module
N_P	parallel branches in a module
N_M	modules in series in an array
N_B	parallel branches in an array
T_a	ambient temperature (°C)
T_c	cell temperature (°C)
G_a	irradiance (W/m^2)
R_s	series resistance (Q)
η	diode ideality factor
K	Boltzmann constant, if $= 1.381 \times 10^{-23}$ (J/K)
FF	Fill Factor

and explanation capabilities that are useful to deal with strong nonlinearities and complex systems (Mellit and Kalogirou, 2008). Mummadi et al. proposed an ANN-based identification of the optimal operating point for a DC motor supplied by PV generator (Veerachary and Yadaiah, 2000). Theodore et al. proposed a MPPT for solar vehicle based on ANN reference voltage estimation (OCRAN et al., 2005). Bahgat et al. proposed a neural network based MPPT for a PV module supplying a DC motor that drives an air fan (Bahgat et al., 2005). Preliminary results show high MPPT efficiency for such methods (Hohm and Ropp, 2003). On the other hand, neural networks are still considered as unstable learning model regarding to the presence of noisy sets, large training set, underfitting and overfitting problems that causes a lack of generalization and trapping on local minima solutions (Gao et al., 2005; Anguera et al., 2007). Moreover, due to the high nonlinearity and close dependence on weather conditions of PV generators, a neural network based model requires the use of a rich training set covering a wide range of climatic conditions which leads to a delicate generalization ability.

This paper presents a new MPPT methodology based on a more robust estimator consisting of multi-model machine learning. The multi-model approach defines a set of three models by means of fuzzy classification, each model consists of a single ANN that emulates the behavior of the PV generator for a specific climatic conditions, so-called "class". The proposed classifier consists of transparent rules-based fuzzy classifier, such rules, unlike opaque or uninterruptable classification is straight forwarded and simple to understand. The multi-model approach aims to decrease the process complexity of the system under wide operating conditions frame, therefore the proposed estimator offers a distinct improvement regarding to the generalization capability comparing to the single ANN estimator. Moreover, the proposed neuro-fuzzy predictor can be successfully implemented for a real time MPPT that can handle rapid weather conditions variations while a P&O algorithm approach and a historical meteorological data based prediction, yet easier to implement but usually fail in case of sudden weather conditions variation.

2. Overview of the grid-connected PV system

Fig. 1 shows the overall of the studied system, composed of a 20 kW photovoltaic generator connected to the main electric grid via two power electronics stages. The first stage consists of a DC–DC converter that insures impedance adaptation between the generator and the load by tracking the reference voltage estimated by the neuro-fuzzy network. While the second stage is composed of a DC bus and a PQ inverter that injects the power generated by the PV generator into the main grid, where the inverter is acting as power controller ensuring a high power factor. In the following subsections, all the components of the grid-connected PV system are described in details.

2.1. Photovoltaic system

The studied grid-connected PV system comprises a 20 kW photovoltaic generator installed at the Engineering Campus of the Tokyo University of Agriculture and Technology (Fig. 2). A dynamic simulation model of the photovoltaic system is designed under Matlab Simulink® environment to analyze the behavior and the performances of the proposed MPPT algorithm.

2.1.1. Simulation model of a PV generator

A simple equivalent circuit for a PV cell (Fig. 3a) consists of a real diode associated to a parallel ideal current source delivering a proportional current to the solar irradiance, from where the following relations can be expressed (Chaouachi et al., 2009):

$$I = I_{SC} - I_d \tag{1}$$

$$\text{where} \quad I_d = I_0(e^{eV_d/\eta KT_c} - 1) \tag{2}$$

$$\text{Therefore} \quad I = I_{SC} - I_0(e^{eV_d/\eta KT_c} - 1) \tag{3}$$

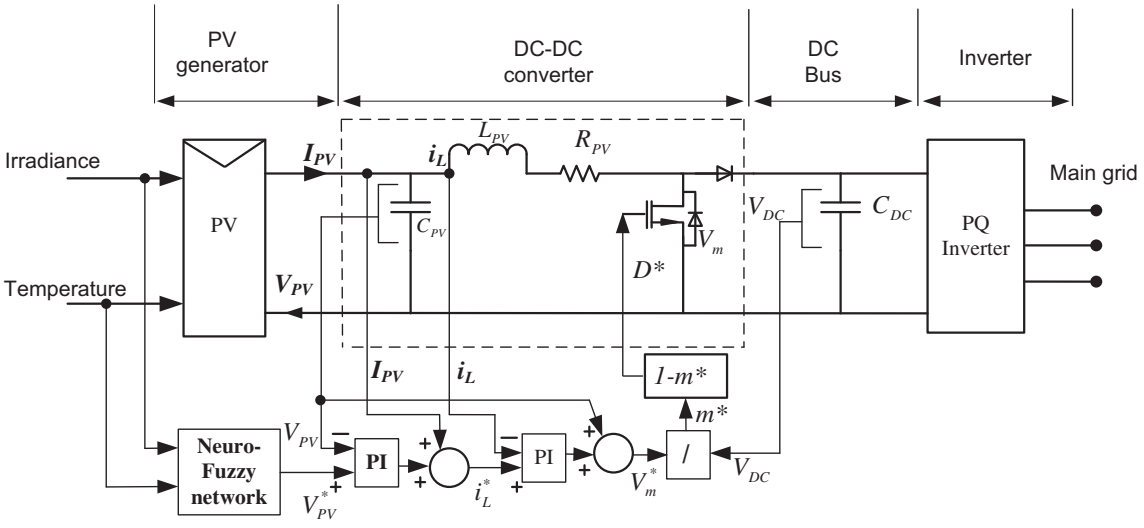

Fig. 1. Overview of the neuro-fuzzy MPPT grid-connected photovoltaic system.

Fig. 2. The studied photovoltaic field installed at Tokyo University of Agriculture and Technology.

To deal with the dynamic behavior of a PV generator, some parallel leakage resistance R_p and a series resistance R_s (associated to the resistance of the semiconductor) should be included (Fig. 3a). However, for the proposed simulation, taking into account both of series and parallel resistances results in computational limitations subjected to the implicit nonlinear nature of the simulation model. Therefore, such approach is usually avoided in the photovoltaic systems bibliography. For the proposed simulation model, the parallel resistance is neglected while the series resistance R_s is considered which represents the internal resistance and the connections between cells. The mathematical relations established afterwards describing the PV generator model is expressed as following:

$$I = I_{SC} - I_0\left\{exp\left(\frac{e(V + I \cdot R_s)}{\eta K T_c}\right) - 1\right\} \tag{4}$$

Considering the case of a photovoltaic generator module (panel), composed of N_P parallel branches, each including N_S solar cells associated in series, the current delivered by a photovoltaic module under constant weather conditions can be expressed as:

$$I^M = I^M_{sc}\left[1 - exp\left(\frac{V^M - V^M_{oc} + R^M_S \cdot I^M}{N_S \cdot V^C_T}\right)\right] \tag{5}$$

The module current has an implicit expression depending on the following variables expressed in function of a single cell parameters:

Short circuit current	$I^M_{SC} = N_P \cdot I^C_{SC}$
Open circuit voltage	$V^M_{oc} = N_S \cdot V^C_{oc}$
Thermal voltage in the semiconductor	$V^C_T = mKT_c/e$
Equivalent serial resistance of the module	$R^M_s = R^C_s \cdot N_P/N_S$

As the first step, under the assumption that all the PV cells are identical, the fundamental simulation parameters for a

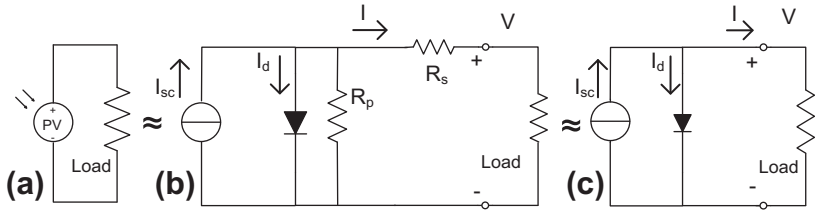

Fig. 3. (a) PV generator model, (b) Equivalent circuit with added R_p parallel and R_s series resistance (c) photovoltaic generator equivalent simple circuit.

solar cell (in standard conditions) are expressed using the module characteristics provided by the manufacturer's catalogue (Appendix A):

$$P^C_{max_o} = \frac{P^M_{max_o}}{N_S N_P} \tag{6}$$

$$V^C_{oc_o} = \frac{V^M_{oc_o}}{N_S} \tag{7}$$

$$I^C_{sc_o} = \frac{I^M_{sc_o}}{N_P} \tag{8}$$

Now, the instantaneous series resistance of a solar cell can be expressed as:

$$R^C_S = \left(1 - \frac{FF}{\frac{P^C_{max_o}}{V^C_{oc_o} I^C_{sc_o}}}\right) \cdot \frac{V^C_{oc_o}}{I^C_{sc_o}} \tag{9}$$

where FF is the Fill Factor and is given by:

$$FF = \frac{\left(\frac{V^C_{oc_o}}{V^C_{T_o}} - Ln\left(\frac{V^C_{oc_o}}{V^C_{T_o}} + 0.72\right)\right)}{\frac{V^C_{oc_o}}{V^C_{T_o}} + 1} \tag{10}$$

Operating condition parameters can be calculated for a fixed voltage V^M, temperature T_a and irradiance G_a using the cell parameters in standard conditions. The short circuit current is proportional to the irradiance and can be expressed as:

$$I^C_{SC} = \frac{I^C_{SC_O}}{G_{a_o}} \cdot G_a \tag{11}$$

The open circuit voltage of the cell is depending on the nominal open circuit voltage and the actual weather conditions which can be expressed using the following relation:

$$V^C_{oc} = V^C_{oc_o} + 0.03 \cdot (T_a + 0.03 \cdot G_a - T_{C_o}) \tag{12}$$

Now, the instantaneous current debited by a photovoltaic module can be finally expressed for the fixed parameters (V^M, T_a, G_a):

$$I^M = N_P \cdot I^C_{SC}\left[1 - \exp\left(\frac{V^M - N_S V^C_{oc} + I^M R^C_S \frac{N_S}{N_P}}{N_S V^C_T}\right)\right] \tag{13}$$

Considering the case of a photovoltaic array that consists in N_B parallel branches, each containing N_M modules associated in series. For a V^M applied voltage, the array current is equal to $I = \sum_{i=1}^{N_B} I^M_i$. If we assume that all the panels are identical and under the same temperature and irradiance, then the total current generated by the array can be expressed as following:

$$I = N_B \cdot I^M \tag{14}$$

2.1.2. Influence of temperature and irradiance on PV operating

Fig. 4 shows the behavior of a photovoltaic panel simulation in accordance to temperature and irradiance

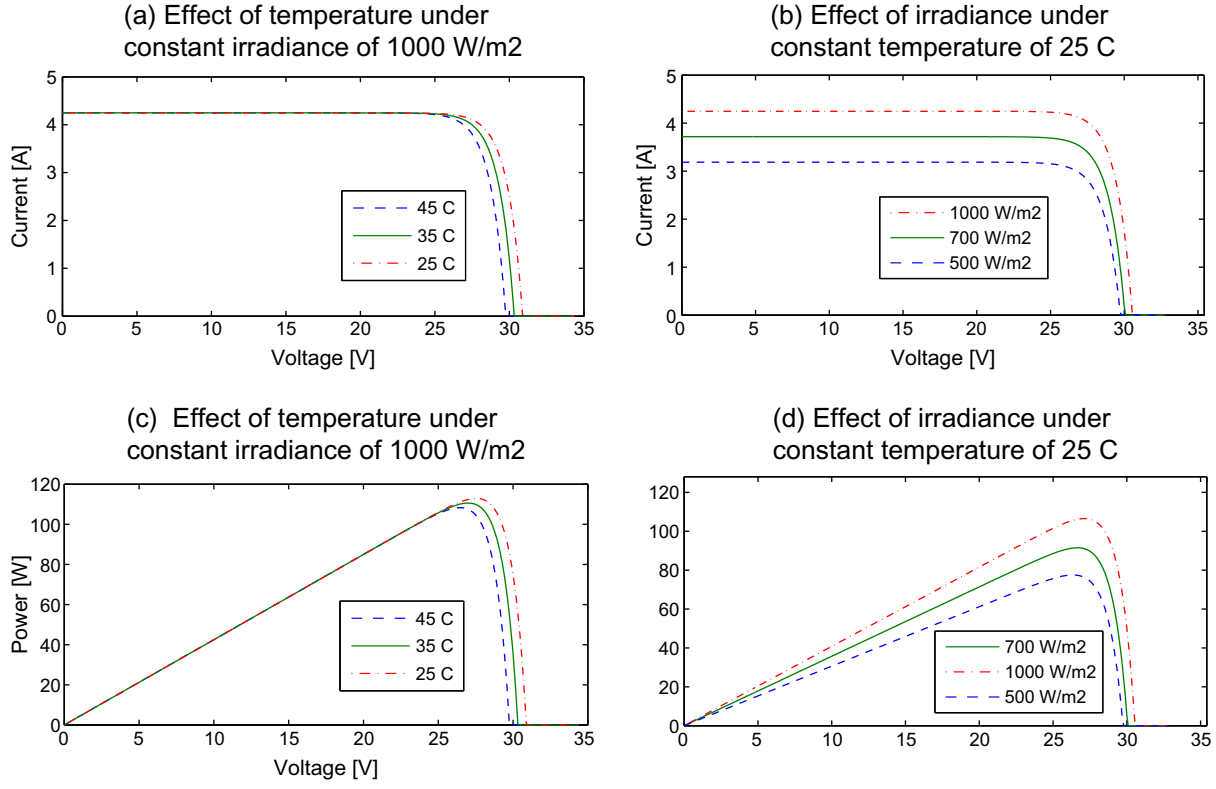

Fig. 4. Temperature (a) and irradiance (b) effects on the IV curve of a PV generator temperature (c) and irradiance (d) effects on the power curve of a PV generator.

variations under respectively constant irradiance and temperature. In fact, a PV generator connected to a load can operate in a large margin of current and voltage depending on weather conditions (Masters, 2004). Fig. 4 shows that the open circuit voltage is increasing following a logarithmic relationship with the irradiance and decreasing slightly as the cell temperature increases. On the other hand, the short circuit current is linearly depending on the ambient irradiance in direct proportion, while the open circuit voltage decrease slightly as the cell temperature increases.

Therefore, the maximum power that could be generated by a PV system is slightly depending on the temperature and irradiance variations: the maximum power increases as the irradiance increases and vice versa, on the other hand a PV generator performs better for low temperature than raised one.

2.2. DC–DC boost converter

The operating point of a PV generator connected to a load is the intersection of the load curve and the PV current–voltage characteristics. In case of resistive load, the load characteristic is a straight line with slop $e(I = \frac{1}{R}V)$, while the power delivered to the load depends on the value of the resistance only. It should be pointed out that if the load R is equal to a certain optimal load R_{opt}, the PV generator delivers the maximum power (MP). However, if the load R is noticeably larger or smaller than R_{opt} the PV generator operates respectively as constant voltage source or constant current source.

To overcome this undesired effects on the PV power output, an electrical tracking have to be achieved through a power conditioning converter (DC–DC converter) inserted between the load and the source to insure an impedance adaptation by matching the load impedance with the varying PV source. In other words, the DC–DC boost converter is used to maximize the energy transfer from the photovoltaic generator to an electrical system by adjusting the PV generator output voltage to a reference value (V_{ref}) at which the PV generator supplies the maximum power.

The proposed DC–DC converter includes two power accumulation elements and thus two controllable variables which are the V_{pv} voltage and the inductor current (i_L), a mathematical model describing the DC–DC converter can be expressed in the following relation (Kamel et al., 2009):

$$\begin{pmatrix} V_m \\ i_{dc} \end{pmatrix} = m \begin{pmatrix} V_{DC} \\ i_L \end{pmatrix} \tag{15}$$

where $m = 1 - D$ and D is the duty cycle of the converter switch expressed as:

$$D = \frac{t_{on}}{T} = t_{on} f_s \tag{16}$$

where f_s is the switching frequency of the converter switch, t_{on} the time which the switch is turned on during a complete period T.

$$\frac{di_L}{t} = \frac{1}{L_{pv}}(V_m - V_{pv}) - \frac{R_{pv}}{L_{pv}} \tag{17}$$

$$\frac{dV_{pv}}{dt} = \frac{1}{pv}(i_L - i_{pv}) \tag{18}$$

The voltage control loop with the PV current compensation gives the reference current i_L^* that can be calculated using Eq. (17):

$$i_L^* = PI(V_{pv}^* - V_{pv}) + i_{pv} \tag{19}$$

where V_{pv}^* is the reference voltage calculated by the neuro-fuzzy logic controller (Fig. 1), PI is the parameters of the proportional-integral controller

The optimal switching voltage is expressed using (18) and (19):

$$V_m^* = PI(V_{pv}^* - V_{pv}) + V_{pv} + \frac{R_{pv}}{L_{pv}} i_L \tag{20}$$

The controller parameters are chosen to maintain constant PV voltage and to minimize the current ripple. The DC–DC converter command is obtained by the inversion of Eq. (15), expressed as following:

$$m^* = \frac{V_m^*}{V_{DC}} \tag{21}$$

With optimal duty cycle $D^* = 1 - m^*$.

A DC link insures an energy balance between the power generated by the PV generator and the power injected into the network by charging or discharging the capacitor, that oscillate between two levels depending on the actual climatic conditions and the power injected.

2.3. PQ inverter

The inverter plays a vital role in grid-connected systems, by interfacing the PV generator with the main utility power system, the configuration of a basic inverter connected to a PV generator is shown in Fig. 5.

The basic and minimum requirement of voltage source inverter is to control the flow of active and reactive power between the PV source and the main utility, the mathematical relations for P&Q magnitudes can be expressed as following in Eqs. (22) and (23) Lasseter et al., 2000:

$$P = \frac{VE}{wL}\sin(\delta_V - \delta_E) \tag{22}$$

$$Q = \frac{V^2}{wL} - \frac{V}{wL}\cos(\delta_V - \delta_E) \tag{23}$$

As the main objective of the current work is to analyze the MPPT proposed methodology during steady-state operation, it would be of no advantage to consider the details of inverter switching. Moreover, if such details are considered, then extra efforts should be done to compensate the undesired effects of the generated harmonics that leads to more heavy computational simulations. Thus, the proposed inverter is represented by its control function while the fast transients related with the commutations of

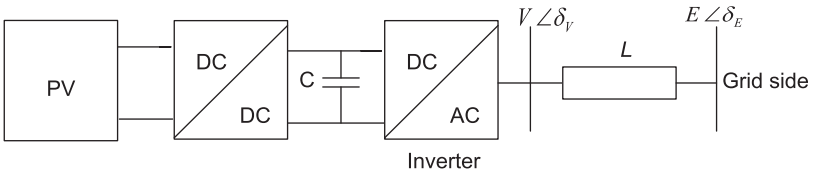

Fig. 5. Basic inverter connected to a PV generator.

the switches are not considered, therefore the power injected at the AC side does not include harmonics, losses or delays. The inverter voltage is represented using the following three controlled sinusoidal voltage sources defined as:

$$V_a = \sqrt{2}V \cdot \sin(wt + \delta_V) \tag{24}$$

$$V_b = \sqrt{2}V \cdot \sin\left(wt + \delta_V - \frac{2\pi}{3}\right) \tag{25}$$

$$V_c = \sqrt{2}V \cdot \sin\left(wt + \delta_V + \frac{2\pi}{3}\right) \tag{26}$$

where the control variables are V and δ_v

The basic structure of PQ inverter controller is shown in Fig. 6, two PI controllers would suffice to control the flow of active and reactive power by generating the proper values of voltage (V) and angle (δ_v) based on the instantaneous value of voltage and current. The reference power (P_{ref}) in Fig. 6 represents the amount of active power produced by the photovoltaic generator interfaced to the main utility through the inverter, while Q_{ref} represents the amount of reactive power desired to be injected into or absorbed from the main utility. In the present case, the inverter is operating at unity power factor ($Q_{ref} = 0$) therefore no reactive power is exchanged and the total MP extracted from the PV generator is injected to the grid.

3. Neuro-fuzzy maximum power point estimation

The neuro-fuzzy network consists of two stages; the first one is a fuzzy-rule-based classifier while the second one is composed of three multi-layered feed forwarded ANNs (Fig. 7). The three ANNs have similar architecture, composed of three layers: input, hidden and output layers.

3.1. Fuzzy rules-based classification

Classification task consists of assigning a class C_j from a predefined class set $C = \{C_1, C_2, \ldots, C_M\}$ to an object belonging to a certain feature space $x \in S^N$, so the problem comes to find a mapping defined as (Kuncheva, 2000):

$$D : S^N \rightarrow C$$

A fuzzy rule-based classification system is composed of fuzzy reasoning method (FRM) and a Knowledge Base (KB) consisting in rule base (RB) and data base that

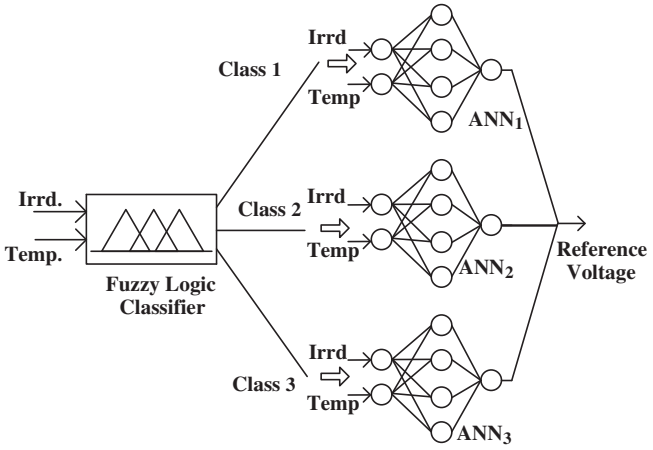

Fig. 7. Architecture of the Neuro–fuzzy network.

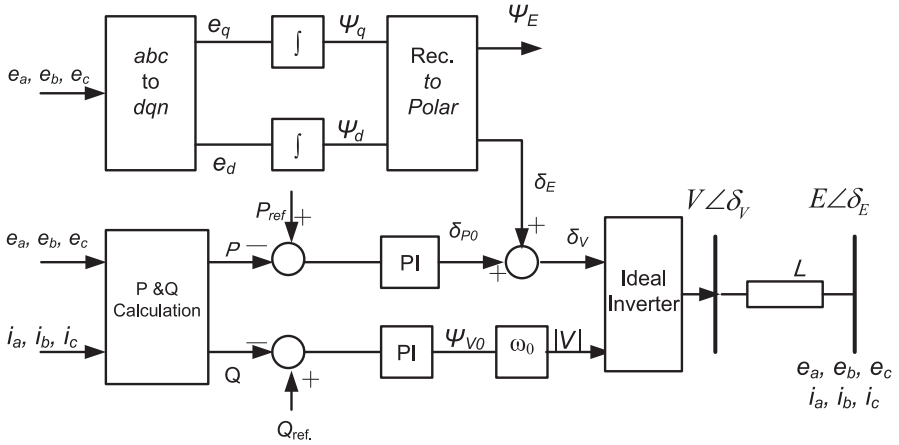

Fig. 6. Basic structure of the inverter PQ control scheme.

describes the semantic of the fuzzy subsets associated to linguistic labels on the if-then part of the rules. Basing on the KB, the FRM determines a label class for admissible patterns as shown in Fig. 8 (Cordon and Jesus, 1999).

Let us consider a rule base $R = \{R_1, R_2, \ldots, R_L\}$ and r_j rules in R, the RBs are generated based on fuzzy rules with a class in the consequent according to the following structure:

$$R_k \quad \text{if } a_1 \text{ is } L_1^k \text{ and } \ldots a_N \text{ then } O \text{ is } C_j \tag{27}$$

where $a_1, \ldots, ,a_N$ is the outstanding selected features for the classification task, $L_1^k, \ldots, L_N^k$ is the linguistic labels to discretize the continuous domain of the variables, O is the class C_j to which the pattern belongs.

3.1.1. Fuzzy reasoning method

A fuzzy reasoning method is an inference procedure that derives conclusions from a set of *if-then* rules and a pattern, such methodology aims to improve the generalization capability of a classification system (Kuncheva, 2000). While each rule r_j in R generates a class C_j related to a pattern $P^t = (p_1^t, \ldots p_N^t)$, the FRM considers the rule with the highest combination between the matching degree of the pattern with the *if-then* part and the certainty degree for the classes. In fact, for each class C_j, the association degree of the pattern with the class O_j can be expressed as following:

$$O_j = max_{k \in L} R^k(P^t) \tag{28}$$

where $R^k(P^t)$ is the strength of activation (matching rule) associated to the kth rule, obtained by applying a t-norm to the degree of satisfaction of the inputs patterns to the clause (a_1 is L_1^k):

$$R^k(P^t) = T(\mu_{L_1}^k(p_1^t), \ldots, \mu_{L_N}^k(p_N^t)) \tag{29}$$

Finally the classification for the pattern E^t is the class C_h such expressed in:

$$O_h = max_{j=1,\ldots,M} O_j \tag{30}$$

This approach can be graphically represented by Fig. 9.

3.1.2. Fuzzy controller design

The fuzzy rule-based classifier was build and designed under the Matlab Fuzzy Logic Toolbox and lately exported into Simulink environment as a part of the neuro-fuzzy network and the whole simulation system.

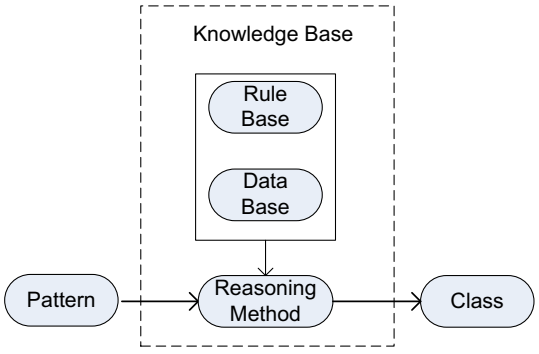

Fig. 8. Fuzzy rule-based classification system.

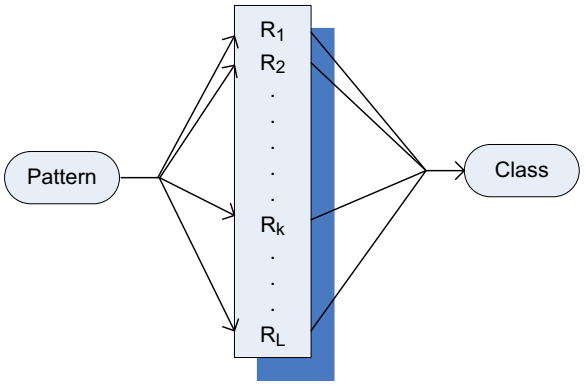

Fig. 9. Fuzzy reasoning method.

3.1.2.1. Membership functions. A membership function is a curve that defines how each point in the input or output space is mapped to a membership value between 0 and 1. Fig. 10a and b shows the temperature and irradiance membership functions in trapezoidal shape. The temperature membership function is sorted into three categories labeled as: hot, warm and cold, while the irradiance membership function is sorted into three categories labeled as sunny, normal and cloudy.

The output of the fuzzy system is the class associated to the inputs pattern. Fig. 10c shows the output membership function in triangular shape, sorted into three categories: class1, class2 and class3.

3.1.2.2. Fuzzy rules. The influence of climatic conditions on the model or behavior of a PV generator can be interpreted through linguistic conditional statements that describe the correlation between the climatic conditions and the PV operating behavior. Indeed, *if-then* statement based transparent rules, similar to those used in fuzzy control (Lee, 1990) are established based on human expertise on the influence of weather conditions on PV systems operating characteristics that are summarized in Table 1.

Fig. 11 shows the clustering output of the fuzzy classifier as a function of output power, the training data set was split into three classes each one is used for the training process of its appropriate ANN. Unlike conventional crisp classification, the proposed fuzzy classifier presents several patterns with similar power level that are classified into dissimilar classes as they belongs to different weather conditions (temperature, irradiance).

3.2. Multi-layred perceptron neural network

Multi-layered perceptrons neural network (MLPNN) has been applied successfully to solve some difficult and diverse problems based on a preliminary supervised training with error back propagation algorithm using an error

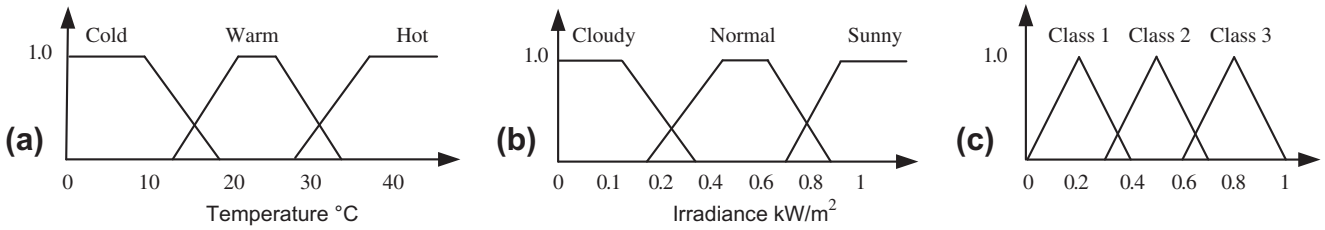

Fig. 10. Inputs and output membership functions of the fuzzy classifier.

Table 1
Fuzzy rules assignment.

Temperature	Irradiance		
	Cloudy	Normal	Sunny
Cold	Class2	Class3	Class3
Warm	Class1	Class2	Class3
Hot	Class1	Class1	Class2

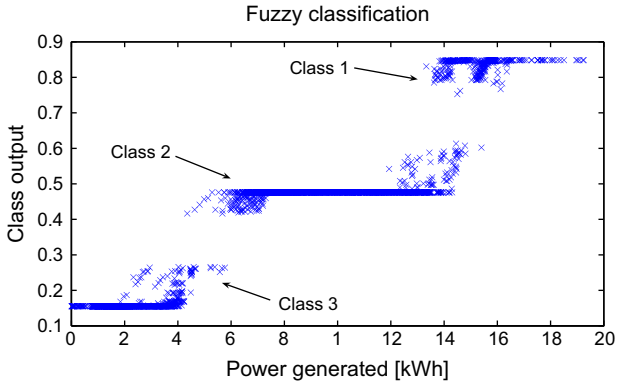

Fig. 11. Clustering of the input patterns (training data).

correction learning rule. Basically, error back learning consists in two pass through the different layers of the network, a forward pass and backward pass. In the forward pass, an activity pattern (input vector) is applied to the sensory nodes of the network, its effect propagates through the network layer by layer to produce an output as actual response. During the backward pass synaptic weights are adjusted in accordance to an error correction-rule. The error signal (subtracted from a desired value) is then propagated backward through the network against the direction of the synaptic connections (Haykin, 1999; Hornik et al., 1989).

To evaluate the performance of the proposed neuro-fuzzy network comparing to a conventional neural network based MPPT method, a single ANN estimator was developed besides the three ANN's (ANN1, ANN2 and ANN3) constituting the neuro-fuzzy learning machine. The networks inputs are temperature and irradiance while the output is the optimal reference voltage.

The training data base was recorded during the year 2008 for the training and testing process the original set was split into three subsets: training set (70%), validation set (15%) used during the training process for early stopping to avoid overfitting problems and testing set (15%) to evaluate the generalization performance of the developed ANNs. To improve the training convergence performances, mean 0 and standard deviation 1 based across channel normalization (Chaouachi et al., 2010) was used for the input training set rescaling, basing on the following relation:

$$S_i = \frac{x_i - \text{mean}}{\sqrt{\frac{\sum_{i=1}^{N}(x_i - \text{mean})^2}{N-1}}} \tag{31}$$

where

$$\text{mean} = \frac{\sum_{i-1}^{N} x_i}{N}$$

x_i the raw input variable X in the ith training case, S_i the standardized value corresponding to x_i, N the number of training case

The target data set was linearly normalized in order to force the network values to be within the range of output activation functions using upper (Y_{max}) and lower bounds (Y_{min}) for the values:

$$Z_i = \frac{Y_i - (Y_{max} - Y_{min})/2}{(Y_{max} - Y_{min})/2} \tag{32}$$

where Y_i the raw target variable Y for the ith training case. Z_i the standardized value corresponding to Y_i.

The backpropagation momentum algorithm was used for the training process of the developed networks, the framework of the ANN's was set out basing on trial and error approach (Table 2). In fact, the networks were trained up to the stopping validation point while their parameters were continuously changed until no significant error performance decrease is observed. It should be noticed that a single hidden layer was sufficient for the proposed task, as adding a second hidden layer did not improve the training performances.

Table 2
Neural networks training parameters.

	ANN1	ANN2	ANN3	Single ANN
Hidden neurons	11	14	11	16
Learning rate	0.1	0.1	0.1	0.2
Momentum	0.3	0.3	0.3	0.35

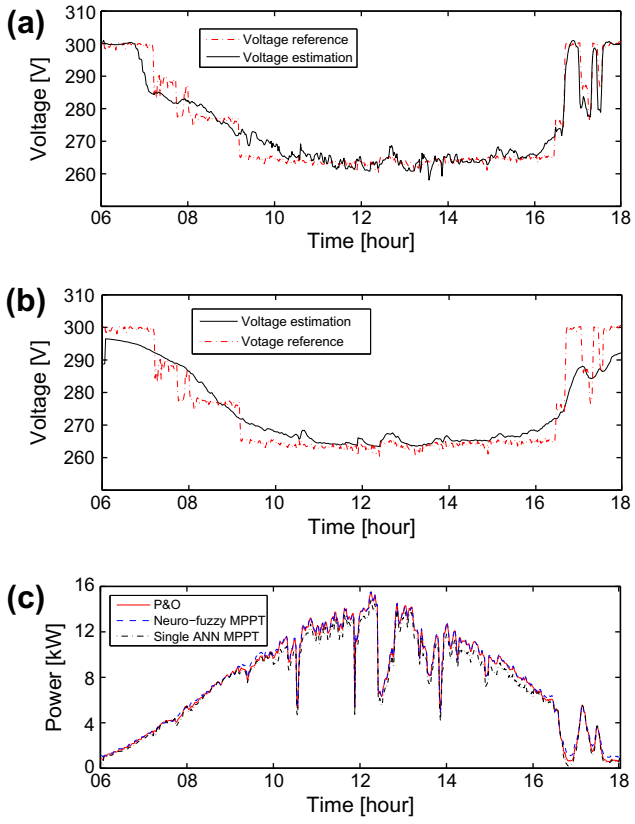

Fig. 12. One day operation performances: (a) Neuro-fuzzy reference voltage estimation. (b) Single ANN reference voltage estimation. (c) Power generation comparison using neuro-fuzzy, single ANN, and P&O algorithm.

4. Simulation results

Several performance criteria are reported in the ANN literature as: the training time, the modeling time and the prediction error. In the present study, as the training process is in offline mode, the first two criteria are not considered to be relevant. Thereby, the estimation performances of the neuro-fuzzy network and the single ANN will be evaluated only in term of estimation error defined as the difference between the experimental and the estimated values based on statistical approach. In fact the mean absolute error (MAE), was applied as statistical error test criteria. On the other hand, the performance of the proposed estimator was compared with the experimental algorithm (P&O) and the conventional ANN estimator regarding to the maximum power extracted during a whole day.

Fig. 12a and b respectively shows the reference voltage estimation by the neuro-fuzzy network and a single ANN comparing to the experimental data for an unsteady weather conditions during a cloudy day. We can see that the proposed machine learning achieved the most accurate estimation. Moreover, for the total testing process mean absolute error for the neuro-fuzzy estimator is 0.139 while the single ANN estimator's error is equal to 2.496. In fact, the complex nature of the PV generator and its nonlinear behavior versus the atmospheric changes involves the use of a large training data base to cover most of eventual weather conditions that leads to classification degradation and loss in the generalization performance caused by overfitting problem. Nevertheless, the proposed neuro-fuzzy

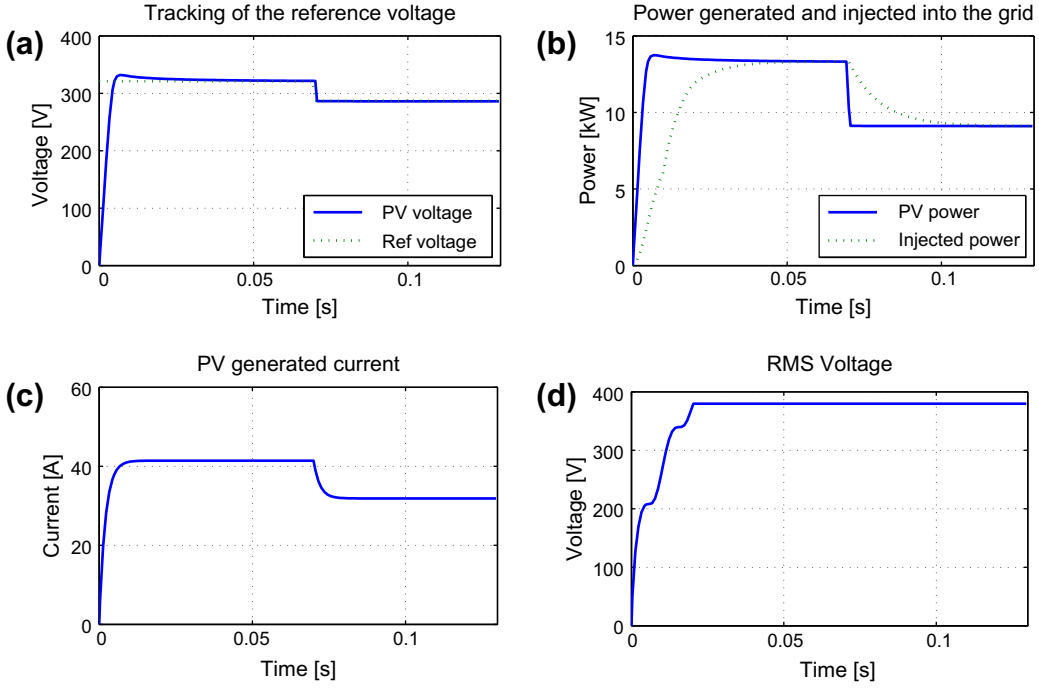

Fig. 13. System operation during a weather condition step: (a) Tracking of the reference voltage. (b) Power generated and injected into the grid. (c) PV generated current. (d) RMS voltage.

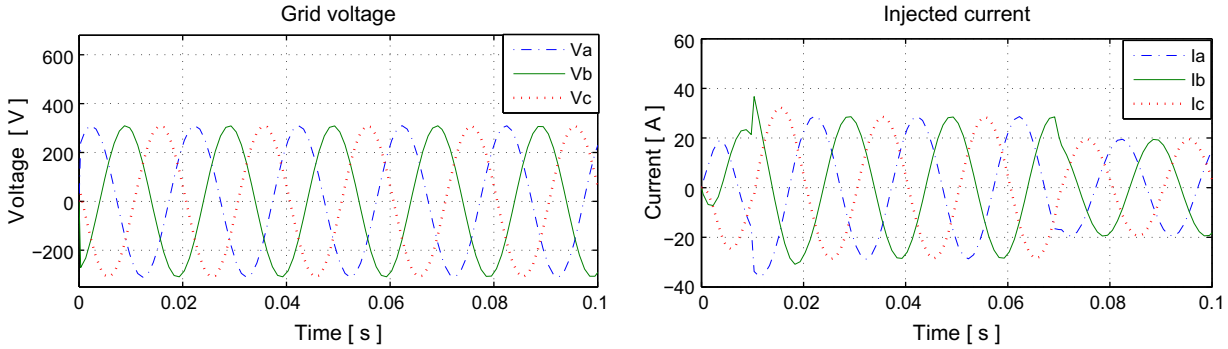

Fig. 14. Grid side voltage and injected current during a weather condition step.

machine learning can overcome these limitations through a better definition of the model complexity based on the fuzzy classification.

Fig. 12c presents the simulation output of the PV system (extracted power) during 1 day using the neuro-fuzzy network and the single ANN comparing to the measured experimental data (P&O). It can be seen that the neuro-fuzzy MPPT methodology accomplished better performances then the single ANN or the P&O's algorithm that can fail to track the MPP or oscillates around it under rapidly changing climatic conditions. In fact, the proposed neuro-fuzzy-based method achieved the highest power efficiency with 6.85% of extra generated power comparing to the single ANN and 2.73% comparing to the experimental dispositive using the P&O algorithm.

In order to validate the stability performances of the proposed MPPT based neuro-fuzzy estimator, we proceeded to observe the tracking of the MP during the grid connection operation. Fig. 13a shows the tracking of the reference voltage estimated by the neuro-fuzzy machine learning after a weather condition step change (irradiance 650 → 500 kW/m^2; temperature 26.5 → 24.5 °C) basing on experimental measures. In fact, the neuro-fuzzy network supplies a new value of reference voltage, tracked through the DC–DC stage so that the overall system can keep operating under optimal conditions, that is to say that the power injected into the main utility is equal to the MP Fig. 13b throughout the steady-state next to the climatic disturbance. Fig. 13c shows the variation of the current generated by the PV array after the climatic perturbation basing on the new set point of the system optimal operation meanwhile the RMS voltage keep stable (Fig. 13d).

Fig. 14 shows the current injected into the main grid and the grid side voltage before and after the weather conditions step change. As it can be seen, the voltage and current are in phase which means that the MP extracted from the PV array can pass into the main grid as the whole system operates at unity power factor ($Q_{ref} = 0$) with no reactive power exchange. The peak occurring approximately at 0.016 s is due to the dynamic state during the initialization of the system (DC–DC converter, DC bus, inverter…). After reaching the steady-state (0.02 s) such peak will not occur even during sudden weather condition changes like the one occurring at 0.07 s.

5. Conclusions

In this paper a new MPPT methodology was applied to a grid-connected photovoltaic system based on a proposed neuro-fuzzy estimator. The whole system was simulated under Matlab Simulink® environment. In this study, the developed neuro-fuzzy network consists of two stages; the first one is a fuzzy rule-based classifier, the second one is composed of three multi-layered feed forwarded ANNs trained offline using experimental data from a real PV system installed at the engineering campus of Tokyo University of Agriculture and Technology. The proposed neuro-fuzzy estimator showed the ability to faithfully emulate the dynamic and nonlinear behavior of a photovoltaic generator under a large wide of climatic conditions. In fact the multi-model aspect of the proposed machine learning confer it a distinct generalization ability comparing to a conventional single ANN-based MPP predictor. Maximum power operation was achieved by tracking the reference voltage estimated by the neuro-fuzzy network through a DC–DC converter. The whole grid-connected system performance was tested during a cloudy day with several rapid irradiance variations. The simulation results showed that the proposed system performances was not degraded, as the MPPT dispositive was able to track the reference voltage insuring an optimal operating condition under any rapid changing meteoric conditions.

Appendix A. PV module specification

Manufacturer	SHARP	Maximum power	120 W
Type	NE-LO1A	V_{OC_o}	30.90 V
Maximum voltage	600 V	I_{OC_o}	4.17 A
Weight	12.50 Kg	V_{pm}	26.70 V

References

Anguera, X., Shinozaki, T., Wooters, C., Hernando, J., 2007. Model complexity selection and cross-validation EM training for Robust speaker diarization. In: Proc of ICASSP.

Bahgat, A.B.G., Helwa, N.H., Ahmad, G.E., El Shenawy, E.T., 2005. Maximum power point tracking controller for pv systems using neural networks. Renewable Energy 30, 1257–1268.

Chaouachi, A., Kamel, R.M., Nagasaka, K. 2009. Modeling and simulation of a photovoltaic field based on matlab simulin. In: Conference on Energy System, Economy and Environment, Tokyo, pp. 70–74.

Chaouachi, A., Kamel, R.M., Nagasaka, K., 2010. Neural network ensemble-based solar power generation short-term forecasting. Journal of Advanced Computational Intelligence and Intelligent Informatics 14 (1), 69–75.

Chua, C.C., Chen, C.L., 2009. Robust maximum power point tracking method for photovoltaic cells: a sliding mode control approach. Solar Energy 83, 1370–1378.

Cordon, O., Jesus, F.H.M.J., 1999. A proposal on reasoning methods in fuzzy rule-based classification systems. International Journal of Approximate Reasoning 20, 21–45.

Enrique, J.M., Duran, E., de-Cardona, M.S., Andujar, J.M., 2007. Theoretical assessment of the maximum power point tracking efficiency of photovoltaic facilities with different converter topologies. Solar Energy 81, 31–38.

Enrique, J.M., Andujar, J.M., Bohorquez, M.A., 2010. A reliable, fast and low cost maximum power point tracker for photovoltaic applications. Solar Energy 84, 79–89.

Esram, T., Chapman, P.L., 2007. Comparison of photovoltaic array maximum power point tracking techniques. IEEE Transactions on Energy Conversion 22 (2), 439–449.

Gao, Z., Ming, F., Hongling, Z., 2005. Bagging neural networks for predicting water consumption. Journal of Communication and Computer 2 (3), 19–24 (Serial No. 4).

Haykin, S., 1999. Neural Networks, A Comprehensive Foundation, Second ed. Springer.

Hohm, D.P., Ropp, M.E., 2003. Comparative study of maximum power point tracking algorithms. Progress in Photovoltaics: Research and Applications, 47–62.

Hornik, K.M., Stinchcombe, M., White, H., 1989. Multilayer feedforward networks are universal approximators. Neural Networks 2 (2), 359–366.

Kamel, R.M., Chaouachi, A., Nagasaka, K., 2009. Design and implementation of various inverter controls to interface distributed generators (DGs) in micro grids. In: Conference on Energy System, Economy and Environment, Tokyo, pp. 60-64.

Kuncheva, L.I., 2000. Fuzzy Classifier Design. Physica-Verlag, Heidelberg.

Lasseter, R. Tomsovic, K., Piagi, P., 2000. Scenarios for Distributed Technology Applications with Steady State and Dynamic Models of Loads and Micro-Sources. CERTS Report.

Lee, C.C., 1990. Fuzzy logic in control systems. IEEE Transactions on Systems, Man & Cybernetics SMC 20 (2), 404–435.

Masters, G.M., 2004. Renewable and Efficient Electric Power Systems. Wiley Interscience.

Mellit, A., Kalogirou, S.A., 2008. Artificial intelligence techniques for photovoltaic applications: a review. Progress in Energy and Combustion Science 34, 574–632.

OCRAN, T.A., Junyi, C., Binggang, C., Xinghua, S., 2005. Artificial neural network maximum power point tracker for solar electric vehicle. Tsinghua Science and Technology 10 (2), 204–208 (ISSN 1007-0214 12/23).

Salas, V., Olias, E., Barrado, A., Lazaro, A., 2006. Review of the maximum power point tracking algorithms for stand-alone photovoltaic systems. Solar Energy Materials & Solar Cells 90, 1555–1578.

Veerachary, M., Yadaiah, N., 2000. ANN based peak power tracking for PV supplied DC motors. Solar Energy 69, 343–350.